

# Conversion of Wood into Hierarchically Porous Charcoal in the 200-gram-scale using Home-built Kiln

*Leonel A. Long<sup>2</sup>, Pablo M. Arnal<sup>1,2,\*</sup>*

1 Facultad de Ciencias Exactas, Universidad Nacional de La Plata. 47 y 115 (1900) La Plata, Argentina

2 Centro de Tecnología de Recursos Minerales y Cerámica (CETMIC), CONICET-UNLP-CICPBA, Camino Centenario y 506, CC 49, B1897ZCA, M. B. Gonnet – La Plata, Argentina.

Corresponding Author:

\* E-mail: arnal@quimica.unlp.edu.ar

## **Abstract**

Wood-to-charcoal is crucial in developing new materials at the lab-scale for relevant applications, such as pollutant removal from water. Unfortunately, laboratory carbonization methods are costly and produce charcoal on the gram-scale. This work presents a simple-to-build and simple-to-operate home-made kiln that carbonizes Eucalyptus wood chips (yield of  $30 \pm 1\%$ ) and produces charcoal on the 200-gram scale. Solid particles had the typical structure, composition, and chemical behavior of charcoal obtained from wood. We believe that this carbonization process eases the charcoal synthesis required for the development of new charcoal-based materials.

## **Key Words**

*Biomass-to-charcoal; home-built kiln; carbonization of wood; synthesis of charcoal; low-tech; simple process; cheap process; reproducible process; Eucalyptus wood; wood-to-charcoal; 200-gram scale synthesis; hierarchical pores; removal of crystal violet; point of zero charge; weak basic chemical groups;*

## Highlights

- Home-built kiln efficiently turns eucalyptus wood into charcoal
- 200-gram scale production of charcoal.
- Cheap and straightforward wood-to-charcoal process.

## 1. Introduction

Conversion of wood into charcoal at a laboratory scale is crucial in developing new materials for everyday uses, such as solid-phase extraction, heterogeneous catalysis, or water potabilization. Charcoals made from wood can have a hierarchical pore structure with macropores ( $50 \text{ nm} < d < 100 \text{ }\mu\text{m}$ ) that facilitate mass transfer throughout the material. Charcoals may also have mesopores ( $2 \text{ nm} < d < 50 \text{ nm}$ ) and micropores ( $d < 2 \text{ nm}$ ) that increase the specific surface area up to  $1000 \text{ m}^2\cdot\text{g}^{-1}$ . Pore walls in charcoals have remarkable chemical stability under many relevant industrial processes (e.g., heterogeneous catalysis, pollutant removal from water) and contain diverse unsaturated organic groups containing mainly C. However, some chemical groups are also containing O and H in a much smaller proportion. The surface chemistry of charcoals can be fine-tuned by changing chemical groups at the interphase between pore walls and fluid within pores. The wall develops a higher affinity for specific molecules in the solution.

At a laboratory scale, wood has been converted into charcoal mainly with relatively expensive processes. These processes involve hardware such as glass (quartz) tubes heated with tubular ovens either under vacuum or the flow of inert gas (e.g., He, N<sub>2</sub>) that produces charcoal on the 1-gram scale. So, the cost of production and gram-scale outputs have been limiting the research of charcoal-based materials. Costs have been impeding access to equipment sometimes. Other times, a few grams of charcoal have not been enough to synthesize new materials and adequately test them afterward.

This work shows that a cheap, home-built kiln converts Eucalyptus wood chips into charcoal at the hundred-gram scale. During the study, we sought evidence by first comparing the yield of our carbonization process and then the properties (inner structure, composition, and chemical behavior in water) of the solid product with those reported in the literature.

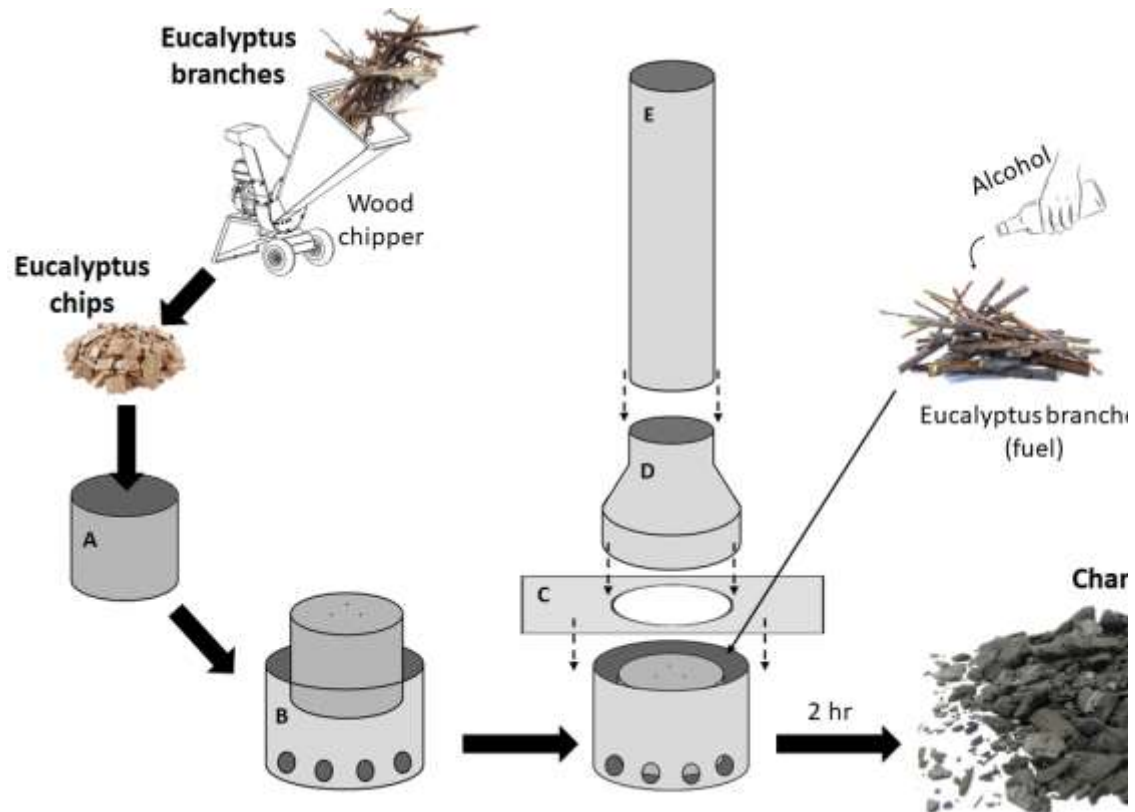
## 2. Materials and Methods

**Chemicals.** NaNO<sub>3</sub> (BIOPACK). Distilled water. HNO<sub>3</sub> 65% solution (Cicarelli). NaOH (S). Crystal violet (S) (Sigma, analytical grade).

**Chips of Eucalyptus Wood.** Eucalyptus branches were collected in the campus of CETMIC. After cutting leaves, branches were chipped (Oy Santasalo-Sohlberg Ab, Helsinki 50) (Scheme 1). Wood chips were stored in an open box until treatment in a home-built kiln.

**Carbonization of Eucalyptus Wood Chips with Home-built Kiln.** Scheme 1 describes the carbonization process. The small metallic cylinder (A) was filled with wood chips. After covering with the big metallic cylinder (B), both cylinders were turned upside down, avoiding wood chips leaving the small cylinder. After filling the space between both cylinders with Eucalyptus branches and adding ethanol (50 mL), branches were set on fire. Elements C, D, and F (Scheme 1) were immediately positioned. Every 30 min, Eucalyptus branches were added to keep the fire burning. Two hours after the ignition of the fire, elements C, D, and F were removed, the fire was put out with distilled water (2 L). After pouring distilled water, elements A and B cooled down to room temperature. Once cooled down to room temperature, elements A and B were turned upside down (ashes and partially combusted branches fell). The big cylinder was removed, and the black solid in the small cylinder was dried (electric furnace, 60 °C, 1 day). The dried, black solid was milled (10-L, plastic jar with screw cap; 25 ceramic balls (3 cm); 30 min) and sieved (ASTM #30 & #60, 250-600 μm). Sieved particles —from now on, charcoal for the sake of simplicity— were stored in closed plastic bags until use after mixing all three samples (synthesis was performed by triplicate). A thorough description of elements A to F is given in Supplementary Information.

**Scheme 1.** Schematic representation of the Wood-to-charcoal process with the home-built kiln.



### Structural Characterization of Solid Product.

*Photography.* The black solid obtained with the kiln before sieving was photographed (Motorola G4 Play).

*Scanning Electron Microscopy (SEM) Images.* Images were obtained from the powder obtained after sieving (JEOL JCM-6000 Neo Scope).

*Hg Porosimetry.* Powder was dried before measurement (110 °C, 24 h) of the Hg porosimetry isotherms (Pascal-Thermo Fisher Module 440 & Module 140). Accumulated specific pore volumes were calculated (SOL.I.D software) between 10 nm and 100 μm. The pore size distribution was calculated from the derivative of the accumulated specific pore volume. The position of the maxima of the distribution curves was estimated with the fit of Gaussian curves.

### Compositional Characterization of Solid Product.

*X-ray Diffraction Analysis (XRD)*. Diffractogram was obtained from dried powders (Philips PW-3710; Cu-K $\alpha$  radiation  $\lambda=0.154$  nm, 35 kV, 40 mA, step  $0.04^\circ$ ,  $2 \text{ s}\cdot\text{step}^{-1}$ ). Reflexes were assigned after comparing the diffractogram with reflexes from a database (Open Crystallographic Database, <http://www.crystallography.net/cod/>, software X'Pert HighScore).

*Thermal Gravimetric & Differential Thermal Analysis (TGA-DTA)*. Measurement was performed on dried charcoal (Rigaku Thermo Plus II; drying  $100^\circ\text{C}$  2 h, 100 to  $1000^\circ\text{C}$  at  $10^\circ\text{C}\cdot\text{min}^{-1}$  under air flow).

*Energy dispersive x-ray spectroscopy (EDX)*. The dried powder was analyzed with EDX (JEOL JCM-6000 Neo Scope) to obtain an elemental composition and mapping of elements. Results were expressed as mass %.

*Fourier Transformed Infrared Spectroscopy Measurements (FTIR) measurements*. Spectra of dried black powder were obtained (Bruker IFS 66).

### **Chemical Characterization of Solid Product.**

*Point of Zero Charge (PZC) Measurements*. The addition method used to obtain the PZC of the black powder has been described previously <sup>[1]</sup>. Briefly, 10 flasks (10 mL, glass, screw cap) were filled with aqueous  $\text{NaNO}_3$  solution (0.3 M). The pH values were adjusted with either  $\text{HNO}_3$  (1 M, 0.1 M, and 0.01 M solutions) or  $\text{NaOH}$  (1 M, 0.1 M, and 0.01 M solutions) to values 2, 3, 4, 5, 6, 7, 8, 9, 10, and 11 (ALPHA, Glass electrode PY-41). Charcoal was added to each flask (ca. 0.2 g measured with  $\pm 0.001$  g precision). Closed flasks were mechanically agitated (Decalab Rotolab-25, 24 h, room temperature  $25^\circ\text{C}$ ). The aqueous solution's pH was measured after exposure to charcoal. PZC was determined from  $\Delta\text{pH}$  (pH values of solution before and after contact with charcoal) vs. initial pH. All experiments were done in triplicate.

*Removal of Crystal Violet from solution in batch systems.* Black powder's ability to remove crystal violet from solution was investigated in batch systems (S/L ratio 10 g.L<sup>-1</sup>) starting at two different concentrations ( $C_1 = 7.9 \pm 0.4$  ppm;  $C_2 = 123.0 \pm 0.4$  ppm). Crystal violet solution (10.00 mL) and charcoal (100.0 mg) were added to 8 flasks (15 mL, glass, screw cap). Closed flasks were mechanically agitated (Decalab Rotolab-25, 25 °C) for  $t = X$  h ( $X = 0.25, 0.50, 0.75, 1, 3, 5, 7$  y 24 for  $C_1$ ;  $X = 0.50, 0.75, 1, 3, 5, 7, 24$  and 48 for  $C_2$ ). After centrifugation (10,000 rpm, 15 min), the concentration of crystal violet in aqueous solution was determined spectrophotometrically (HP 8453, 590 nm). All experiments were done in triplicate.

### **Data Analysis.**

*Yield of carbonization.* The yield of the carbonization process was calculated (Equation 1) from the mass of charcoal ( $m$ ) and of wood chips ( $m_0$ ):

$$Yield = \frac{m}{m_0} 100 \quad (1)$$

*Percentage of crystal violet removed in batch systems.* Percentage of removal of crystal violet from solution in batch systems was calculated (Equation 2) considering the initial concentration  $C_i$  and the concentration at the time  $X$  h ( $C_t$ ):

$$\%Removed = \frac{(C_i - C_t)}{C_i} \cdot 100 \quad (2)$$

*Mean values.* Mean values were expressed as mean value  $\pm$  confidence interval (CI) obtained from ANOVA.

*Comparison of mean values with ANOVA.* Analysis of variance (ANOVA) of point of  $\Delta$ pH and of %removal of crystal violet was conducted (InfoStat version 2020; Centro de

Transferencia InfoStat, FCA, Universidad Nacional de Córdoba, Argentina) ( $\alpha = 0.05$ ). Data normality was verified with Q-Q plot. Variance homogeneity was verified with Fisher test.

*Pair-wise comparison of mean values with Tukey test.* Comparisons among multiple means were made by Tukey test ( $\alpha = 0.05$ ).

### **3.Results and Discussion**

**The process with Home-built Kiln compatible with Carbonization.** Eucalyptus wood chips convert into a black solid with a yield of  $30 \pm 1\%$  ( $n = 3$ ) (see Data in SI). The low dispersion indicates a reproducible process. The mean value is within yield values (28 – 36%) reported for wood carbon with standard laboratory carbonization equipment [2–4]. In contrast, the combustion of Eucalyptus wood has much lower yields (1.9 – 2.9%) [5,6]. Hence, the yield of the process presented here is compatible with a carbonization process.

**Solid Material having Wood-like Structure and Hierarchical Pores.** After grinding and sieving the black solid, a particulate material (250 – 600  $\mu\text{m}$ ) was obtained. These particles have a wood-like structure [7–10] with hierarchical intraparticle pores. Intraparticle pores seem to have a trimodal size distribution. The smallest pores seem to peak at ca. 65 nm, mid-size pores at 2.5  $\mu\text{m}$ , and big pores at 50 – 100  $\mu\text{m}$  (Figure 1 & Figure 2). SEM-images show big pores seem, but Hg porosimetry isotherms do not. The presence of big intraparticle pores seems to overlap with interparticle pores. This inner structure is also characteristic of charcoal obtained from wood with conventional carbonization equipment. Though being a complex process, the carbonization of wood starts with water evaporation below 200 °C. It follows with other condensation reactions that set free more water and other C-containing species. During this process, the lignin present in cell walls seems to preserve the inner structure while cellulose and hemicellulose largely dehydrate.



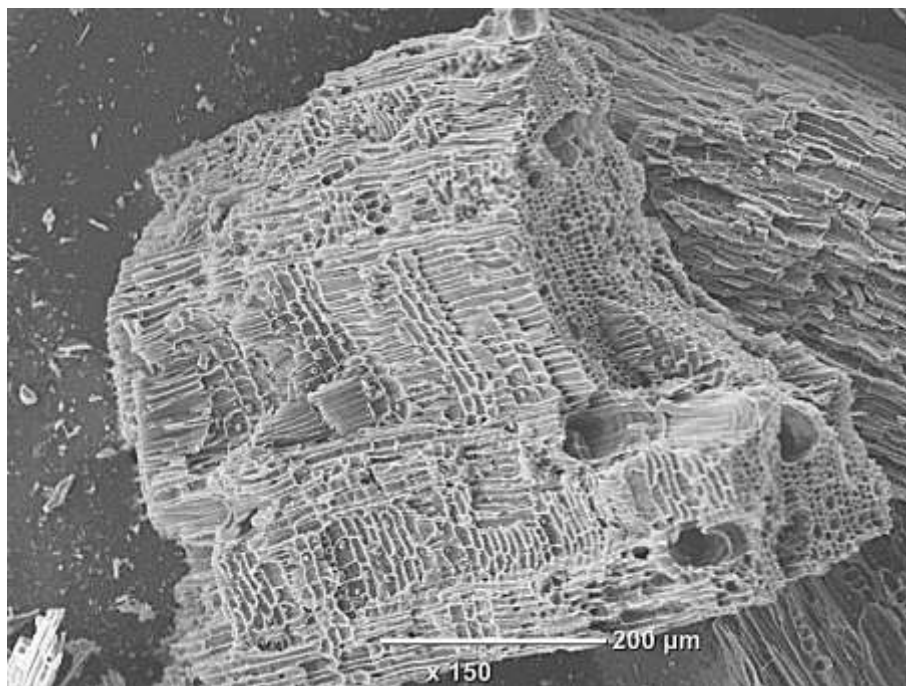


**Figure 1.** Scanning electron microscopy image of the particulate material obtained with the process described in this work.

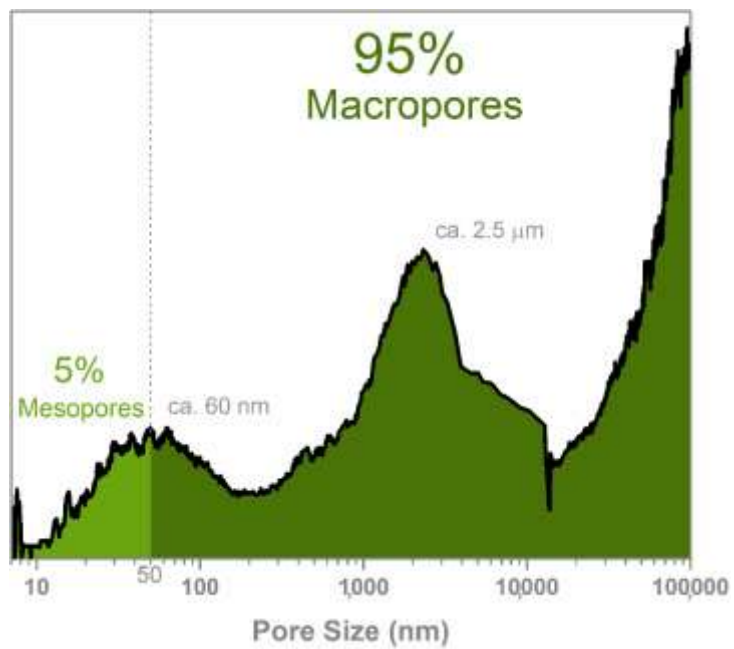


**Figure 2.** Pore size distribution calculated from the Hg porosimetry intrusion isotherm.

**Solid Material with Composition of Charcoal.** The black particulate material has much C (78.8%), some O (14.6%), and a small amount of Ca and K (4.2% and 2.4%, respectively) (EDX). These values may somewhat overestimate the actual elemental composition, as H remains undetected with EDX. However, H contributes little (< 3%) to the composition of carbonized Eucalyptus wood <sup>[11,12]</sup>. For example, if we consider the presence of 3% H, the corrected composition in terms of C and O would be 76.5% and 14.2%, respectively. So, the composition trend remains unaltered for C and O. This trend in composition has been reported for carbonized Eucalyptus wood <sup>[11-13]</sup>.

The solid experienced a drastic mass loss (93.4%) when heated under airflow below 600 °C (Figure 9). Charcoal has been reported to burn when heated in air [14] similarly. This mass loss should originate in the combustion of most black solid.

FTIR spectra show the presence of alkane (3000-2840 (w), 1250-1000 (m)  $\text{cm}^{-1}$ ), alkene (2962-2853 (w), 1650-1500 (m), 1513-1495 (s)  $\text{cm}^{-1}$ ), hydroxyl (3700-3200 (br)  $\text{cm}^{-1}$ ), and carbonyl (1700 (m)  $\text{cm}^{-1}$ ) chemical groups in the solid (Figure 3). These chemical groups may form the backbone of the black particles and are typical for charcoal obtained from wood.

Besides, the black solid contained micrometer-sized  $\text{CaCO}_3$  and  $\text{CaC}_2\text{O}_4$  crystals (Figure 4) scattered throughout the solid particles (EDX, Figure 8 SI). Those crystals are present in Eucalyptus wood. Despite the thermal treatment experienced in the kiln, those crystals also appear in the black solid. These inorganic particles, which are likely trapped within the hierarchical pore structure, have been seen in charcoals obtained with standard laboratory equipment.

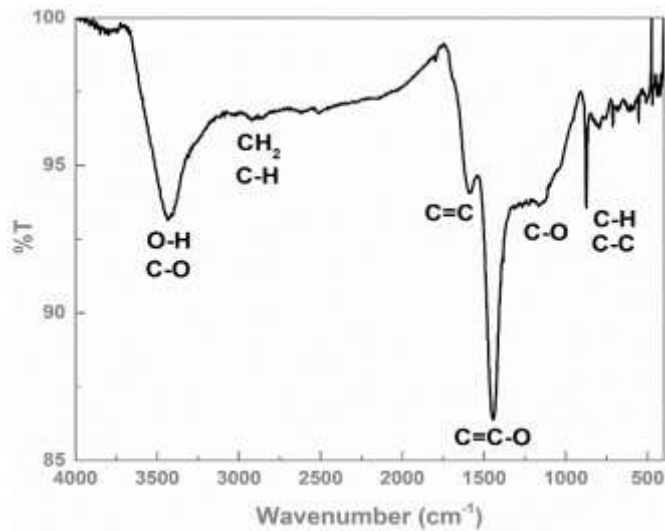


**Figure 3.** FTIR spectrum obtained from the particulate material.

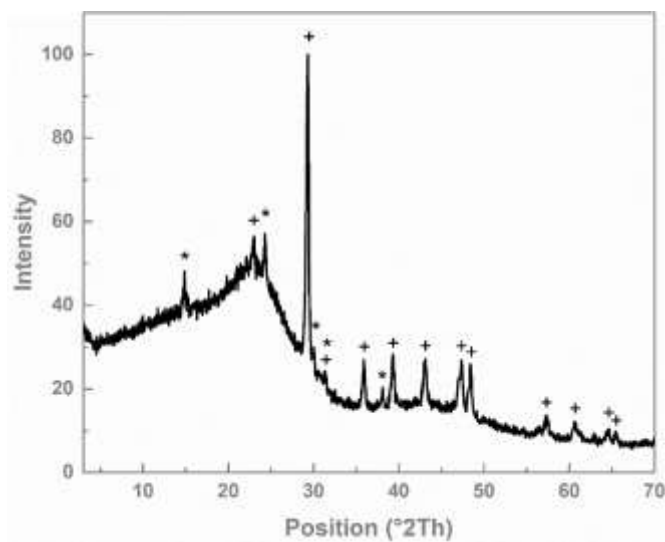


**Figure 4.** X-ray diffractogram obtained from particulate matter. Calcite (+) (Ref Code: 00-035-0914 ICSD) and  $\text{CaC}_2\text{O}_4 \cdot \text{H}_2\text{O}$  (\*) (Ref Code: 00-035-0914 ICSD).

**Solid Material with Surface Chemistry of Charcoal.** When immersed in an aqueous solution, its pH significantly increases for solutions with an initial pH value at 3 – 9, slightly increases for pH = 2, and does not change for solutions with initial pH = 10 – 11 (Figure 5). The pH increment peaks for a solution with initial pH = 4. Also, solutions with initial pH = 4 – 9 end up with final pH values between 9 and 10. In solid particles, weak basic

chemical groups at the surface seem to determine their chemical behavior. At least some basic groups are so weak that they can remove H from water at  $\text{pH} > 7$ . This chemical behavior has been reported for charcoal [15].

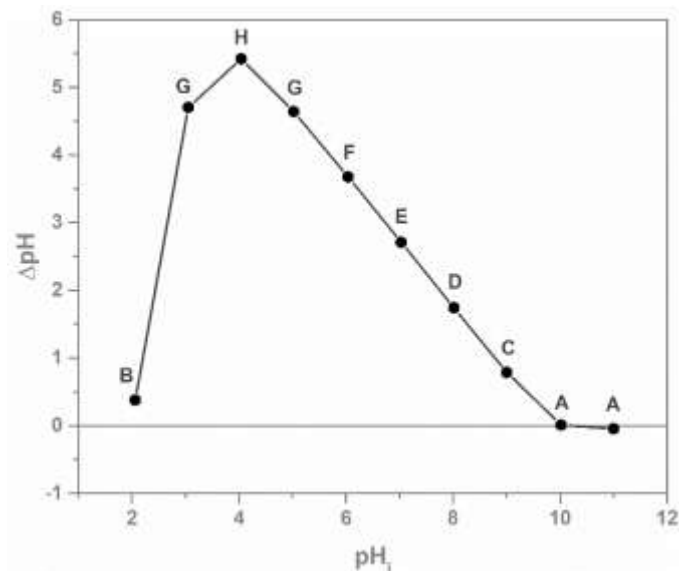


**Figure 5.** Graph  $\Delta\text{pH}$  vs  $\text{pH}$  obtained by Drift Method. Different letters indicate statistically significant difference (Tukey test,  $\alpha = 0.05$ ).

Furthermore, black particles effectively remove (92-97%) crystal violet from aqueous solutions (ca. 1 to 100 ppm initial concentration) (Figure 6). Crystal violet is an organic cation in aqueous solutions sometimes used as a probe molecule to remove pollutants from water [16-18]. The drop in crystal violet in this study's solutions seems to occur because a chemical bonding with surface groups in the black solid has already been observed for charcoal [19,20].

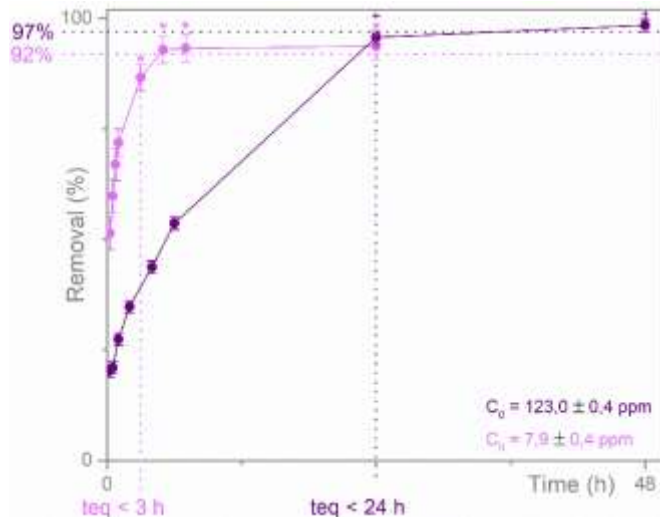


**Figure 6.** Crystal violet removal kinetics on charcoal. Initial crystal violet concentrations were  $7.9 \pm 0.4$  mg/L (light violet) and  $123.0 \pm 0.4$  mg/L (dark violet). The error bars correspond to the confidence interval obtained through ANOVA. Symbols \* and + indicate no statistically significant difference (Tukey Test,  $\alpha = 0.05$ ).

In few words, the home-built oven enables converting Eucalyptus wood chips into charcoal with a simple process.

### Limitations and Strengths of this Study.

The solid's elemental composition was not fully determined. EDX used in this study is unsuitable for the determination and quantification of light elements like H. Because of unsaturated organic groups in carbon, the amount of H is generally small. Though H ought to be quantified to determine the elemental composition of the charcoal, this limitation does not affect the fact that the home-built kiln successfully carbonized wood chips.

Despite its simplicity, the carbonization process presented in this work was highly reproducible. Three independent carbonizations had a yield with low dispersion ( $30 \pm 1\%$ ). The drift method and the removal of crystal violet were also performed in triplicate. Mean values with low dispersions were obtained. The reproducibility of the experiments seems to be a valuable strength.

## **Implication and Future Research.**

We speculate that this study may ease the scientific research with charcoal. Charcoal is now accessible without expensive lab equipment running either in vacuum or with inert gases. Furthermore, charcoal can now be quickly produced in the hundred-gram scale instead of the usual gram-scale (production two-order of magnitude higher!). An easy and chip process is now available to produce charcoal for studies in, for instance, energy storage, heterogeneous catalysis, environmental remediation, and water potabilization [21]. The carbonization process has variables that may be explored to modify the properties of the charcoal (e.g., impregnation of wood chips with  $\text{ZnCl}_2$  or  $\text{H}_3\text{PO}_4$ ; variation of biomass).

## **5. Conclusion**

In summary, this study presents a simple, cheap, and fast carbonization method that enables the production of charcoal on a hundred-gram scale. Though proven with Eucalyptus wood chips, the carbonization process may quickly adapt to other types of woods and plant parts. By easing the carbonization of biomass, this study may facilitate scientific research with charcoal worldwide.

## **6. Acknowledgments**

The authors acknowledge the funding support of *Consejo Nacional de Investigaciones Científicas y Técnicas* (PIP2013-0105 & Doctoral Fellowship of Leonel Long) and *Agencia Nacional de Promoción Científica y Tecnológica* (PICT-2014-2583).

## **7. References**

- [1] H. N. Tran, Y. F. Wang, S. J. You, H. P. Chao, *Process Saf. Environ. Prot.* **2017**, *107*, 168–180.
- [2] K. A. Hina, P. A. Bishop, M. C. A. A, **2010**, 606–617.

- [3] S. Dawood, T. K. Sen, C. Phan, *Desalin. Water Treat.* **2016**, *57*, 28964–28980.
- [4] N. A. de Figueredo, L. M. da Costa, L. C. A. Melo, E. A. Siebeneichlerd, J. Tronto, *Rev. Cienc. Agron.* **2017**, *48*, 395–403.
- [5] S. V. Vassilev, C. G. Vassileva, Y. C. Song, W. Y. Li, J. Feng, *Fuel* **2017**, *208*, 377–409.
- [6] M. J. Antal Jr, E. Croiset, X. Dai, C. DeAlmeida, W. S.-L. L. Mok, N. Norberg, J.-R. R. Richard, M. Al Majthoub, M. J. J. Antal, E. Croiset, X. Dai, C. DeAlmeida, W. S.-L. L. Mok, N. Norberg, J.-R. R. Richard, M. Majthoub, *Energy and Fuels* **1996**, *10*, 652–658.
- [7] A. Fahn, *Anatomía Vegetal*, H. Blume Ediciones, Madrid, España, **1978**.
- [8] K. Esau, *Anatomía Vegetal*, Omega, **1985**.
- [9] T. Nilsson, R. Rowell, *J. Cult. Herit.* **2012**, *13*, S5–S9.
- [10] J. I. Goldstein, in *Wood Struct. Compos.* (Ed.: L. Menachem), Marcel Dekker Inc., New York, Basel, Hong Kong, **1991**.
- [11] M. Kumar, R. C. Gupta, T. Sharma, *Biomass and Bioenergy* **1992**, *3*, 411–417.
- [12] J. Pastor-Villegas, J. F. Pastor-Valle, J. M. M. Rodríguez, M. G. García, *J. Anal. Appl. Pyrolysis* **2006**, *76*, 103–108.
- [13] F. T. M. Silva, C. H. Ataíde, *Energy* **2019**, *172*, 509–516.
- [14] K. Elyounssi, F. X. Collard, J. A. N. Mateke, J. Blin, *Fuel* **2012**, *96*, 161–167.
- [15] H. N. Tran, Y. F. Wang, S. J. You, H. P. Chao, *Process Saf. Environ. Prot.* **2017**, *107*, 168–180.
- [16] R. Ahmad, *J. Hazard. Mater.* **2009**, *171*, 767–773.

- [17] P. Sun, C. Hui, R. Azim Khan, J. Du, Q. Zhang, Y.-H. Zhao, *Sci. Rep.* **2015**, *5*, 12638.
- [18] C. Djilani, R. Zaghdoudi, A. Modarressi, M. Rogalski, F. Djazi, A. Lallam, *Chem. Eng. J.* **2012**, *189–190*, 203–212.
- [19] K. Mohanty, J. T. Naidu, B. C. Meikap, M. N. Biswas, *Ind. Eng. Chem. Res.* **2006**, *45*, 5165–5171.
- [20] P. Sudamalla, M. Matheswaran, P. Saravanan, *Sustain. Environ. Res.* **2012**, *22*, 1–7.
- [21] H. Zhu, W. Luo, P. N. Ciesielski, Z. Fang, J. Y. Zhu, G. Henriksson, M. E. Himmel, L. Hu, *Chem. Rev.* **2016**, *116*, 9305–9374.

## Supplementary Information

### A. Construction of Home-built kiln

1. Prepare elements A and B: Elements A and B of the oven are food cans open on one side and with volumes 2.8 L (height 15.0 cm, diameter 15.5 cm) and 8.7 L (height 23.0 cm, diameter 22.0 cm).
2. Drill three holes in the center of the base of element A with a nail ( $d = 3$  mm) and a hammer (see Scheme 1).
3. Drill holes ( $d = 1.5$  cm) every 3 cm on the side of element B at a distance of 1 cm from the closed edge.
4. Cut out a circle ( $d = 20.0$  cm) in the center of a rectangular metal sheet (40.0 cm by 33.0 cm).



5. Get a truncated metal cone ( $d_{\text{major}} = 21.0$  cm,  $d_{\text{minor}} = 9.5$  cm) (chimney pipe reducer).
6. Get a metallic cylinder ( $d = 10.0$  cm, length = 85.0 cm).
7. Ensemble kiln as indicated in Scheme 1.

#### B. Yield of Carbonization Process

synthesis	$m_0$ (g)	$m$ (g)	yield (%)
1	664.0	205.0	30.87
2	737.0	211.0	28.63
3	730.5	212.3	29.06

#### C. Caracterizaciones del producto sólido



**Figure 7.** Digital photograph of the material obtained supported on a white sheet of paper.

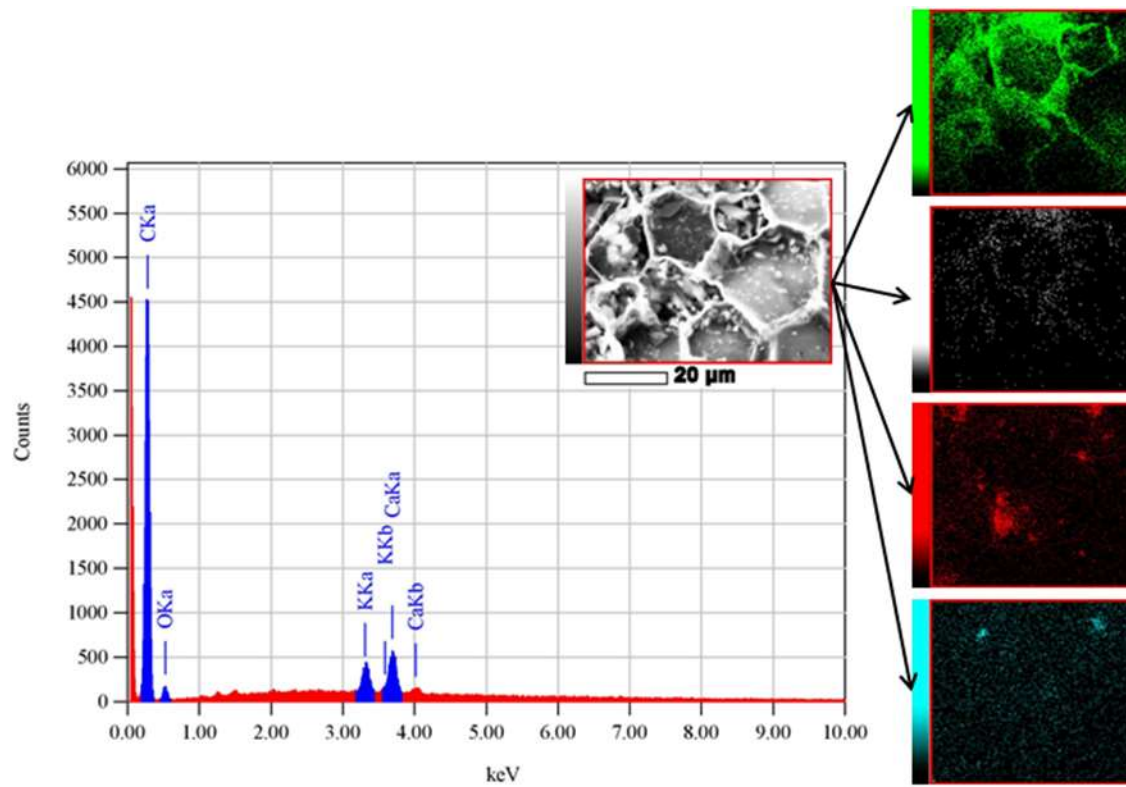


**Figure 8.** Mapping of elements in particulate material using EDX.

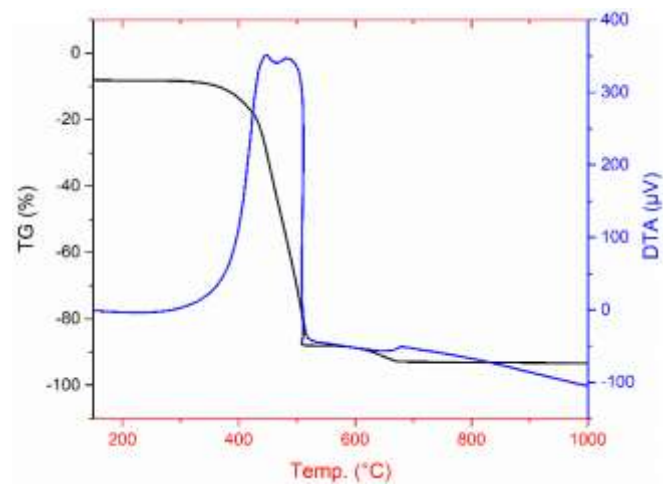


**Figure 9.** TGA-DTA analysis of the black solid produced with the home-built kiln.